International Journal of
Advances in Scientific Research and Engineering (ijasre)

E-ISSN : 2454-8006

DOI: http://dx.doi.org/10.31695/IJASRE.2018.32765

Volume 4, Issue 6
June - 2018

Analysis and Evaluation of Oil Well Riser with Different Exit Geometries Using Computational Fluid Dynamics (CFDs)

Ejiroghene Kelly Orhorhoro[1], Ikpe Aniekan Essienubong[2] and Aregbe Olorunleke[1]

Lecturers [1] and Research Scholar [2]

[1]Department of Mechanical Engineering

College of Engineering, Igbinedion University

Okada, Edo State

Nigeria

[2]Department of Mechanical Engineering

College of Engineering, Coventry University, West Midlands

United Kingdom

ABSTRACT

The exploration of large oil fields or wells in deep waters for crude oil and gas has generated immense challenges within the oil and gas industry that has caused remarkable developments in methods of optimizing production of oil and gas. This research work presents the analysis and evaluation of the flow dynamics of an exit riser configurations using computational fluid dynamics (CFDs). STAR-CCM+ computational fluid dynamics (CFD) tool was employed in this research work. To model the flow in the exit configuration, the geometry of the exit configuration was created using CATIA. The CATIA model saves as IGES format were imported into the STAR CCM+ as regions with the one boundary per face setting, the one region per body setting was also selected and the sewing tolerance was set to 0.001. Four different exit configurations were analyzed for the single phase flow. The results obtained show that the flow in the exit configuration 3 converges faster. Also, from the pressure plot it is discovered that the pressure remained steady until it reaches the junction where a division of the flow occurs. The total pressure and the static pressure are low for exit 3 and lowest for exit 4. For companies where the computational cost is of paramount importance, exit 4 should be considered if oil-field problems and monitoring are done via CFD tools.

Key Words: Oil well riser, Computational Fluid Dynamics, STAR CCM+, CATIA, Pressure.

1. INTRODUCTION

The increased energy demand as well as reduced availability of oil in shallow waters has increase the exploration and production activities for oil and gas in ultra-deep water environments [1-3]. The exploration of large oil fields or wells in deep waters for crude oil and gas has generated immense challenges within the oil and gas industry that has caused remarkable developments in methods of optimizing production of oil and gas in extremely low pressure reservoir, deep water and ultra-deep water offshore operations, the type of equipment, procedures, instrumentation, and remote operations. Of the much advancement in the deep water oil exploration, the oil well riser is an important development [4]. Large volumes of oil and gas have been produced from deep-water basins and there are still several quantities of resources sitting in reserves scattered within ultra-deep waters. Several production optimization methods have been researched and adopted by companies to meet increasing energy demands [5-6]. As the advancement in offshore hydrocarbon exploration in ultra-deep heightens, long risers have evolved. The riser technology is keys in the future of oil and gas field development. Production risers used in deep and ultra-deep water locations are longer than those used in shallow waters. The length of the production riser depends on the depth of the water in which exploration is being

carried out. The depth of the water also determines the pressure required to lift reservoir fluid to the surface [7-8]. To improve deep water exploration, oil and gas engineers are continuously experimenting riser designs that are economical. Despite the advancement in oil and gas production risers, various technical solutions in terms of materials, design and feasibility of riser geometries in ultra-deep waters are still undergoing research for possible improvement in riser performance for future applications [9]. In deep water exploration; riser configurations like steel catenary risers, hybrid risers as well as flexible risers have been used. Significant improvements in these riser configurations are being considered for on-going oil field developments as well as future developments as riser systems represent a substantial portion of the development costs in floating oil and gas production systems [10]. Of the lot, steel catenary risers find application in many recent oil field developments as they represent cheaper alternative to commonly used flexible and rigid risers in floating platform designs. Steel catenary risers can also offer economic solution for riser designs in fixed platforms. This present work will consider steel catenary riser in a bid to evaluate the flow dynamics of the exit riser configurations.

2. RESEARCXH METHODOLOGY

8in (203.2mm) diameter was selected for use in this analysis. This pipe size corresponds to those often found in industrial riser applications. The geometry of the risers in the analysis was constant. The diameters of the pipes being analyzed were allowed to be constant throughout the analysis. The riser is assumed to possess a similar geometry at the entry and at the exit. The lengths of the pipe used for the analysis were chosen such that the changes between the entry and the exit of the pipe can be carefully observed. Since fluid flows in pipes develop over a length of the pipe, the length of pipe used for the analysis is allowed to be greater than the entry length of the flow being analyzed [11]. To model the flow in the exit configuration, the geometry of the exit configuration was created. The model was created in CATIA. The CATIA model saves as IGES format were imported into the STAR CCM+ as regions with the one boundary per face setting, the one region per body setting was also selected and the sewing tolerance was set to 0.001. A careful selection of exit riser configurations was made. Four different exit configurations were analyzed for the single phase flow (Figure 1.1). The geometry of the riser is those available in real life cases. The geometry of the simulated riser was proposed based on existing configurations. STAR-CCM+ computational fluid dynamics (CFD) tool was employed in this research work. It was created by CD-ADAPCO to provide an easy-to-use engineering software/tool for use within the CFD clime. It is prepared in a way to ensure that both first-timers and experts within the CFD discipline can use it. STAR-CCM+ apart from being a CFD solver, is a process for solving flow related problems, heat transfer problems as well as stress problems [12-13].

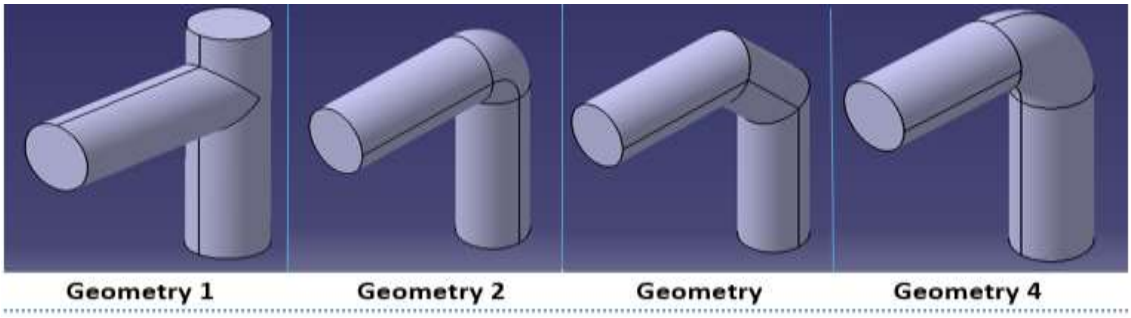

Figure1.1: Exit Configuration Details

i. The first exit configuration is one that has branches as the flow progresses. One of the two branches is completely closed while the other branch is the pressure outlet. It is expected that there would be pressure build up within the system resulting from backflow from the closed branch.
ii. Exit configuration 2 has a sharp corner that is ninety (90) degrees. The bend has a radius that is equal to the radius of the pipe. The configuration is expected to have the same effect as a 90 degrees elbow at the joint.
iii. Exit configuration 3 has a slope that is forty-five (45) degrees in nature. The slope is expected to allow the free passage of the flow with minimal pressure loss considering that the bend is not a very sharp one. The continuity of the bend at the two sharp edges may affect the overall performance of the exit configuration.
iv. Exit configuration 4 has a smooth bend that has no significant effect on the geometry of the pipes. It has a somewhat larger radius that the exit configuration 2. The configuration is expected to ensure easy passage of the flow build-up in the riser.

DOI: 10.31695/IJASRE.2018.32765

Table1.1. Flow Properties for the Single Phase Flow in the Risers

Property (unit)	Value	Remark
Velocity of flow	3.42 m/s	
Density of Crude oil	855kg/m^3	
Reynolds Number of the flow	92659.2	Turbulent
Mach Number of the flow	0.00997	Incompressible
Mass Flow Rate	94.74kg/s	
Turbulence Intensity	0.03831	
Turbulence Length Scale	0.014224m	
Boundary Layer Thickness	0.00234m	
Prism Layer thickness	0.068	Mesh Selection
Prism layer stretching	1.2	Mesh Selection
Number of layers	8	Mesh Selection
Base size	50mm	Mesh Selection
Time	Steady	Physics Selection
Flow	Segregated flow	Physics Selection
Material	Liquid	Physics Selection
Temperature	293K	Boundary condition
Turbulent length scale	7% of the Hydraulic diameter	Boundary condition
Turbulent velocity scale	10% of the free steam velocity	Boundary condition
Reynolds-Averaged Turbulence	K-epsilon	Physics Selection
Space	3D Flow	Physics Selection
Mesh type	Polyhedral (for Volume Mesh) Surface Remesher (Surface mesh) Prism Layer Mesh (For the prism layer)	Mesh Selection

3. RESULTS AND DISCUSSION

In Star CCM+ modelling of flows, the residual plot is significant in monitoring the response of the various flow variables during computation. The momentum and energy calculations are used to determine at what point the computation converges since computation is an approximation of the various governing equations of flow. A steady residual plot is an indication that the flow parameters have converged and are an approximate representation of the various parameters. The simulation can thus be terminated at steady residual values below 1E-4. The plots of the residuals of the flow in the various pipes are shown in Figure 1.2 –Figure 1.5.

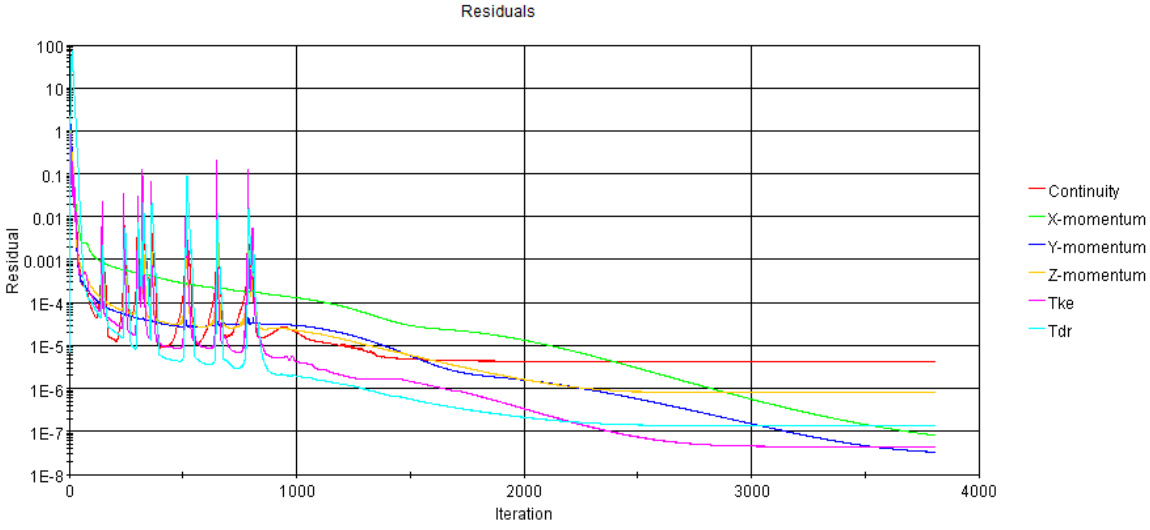

Figure1.2: Residual Plot for Pipe

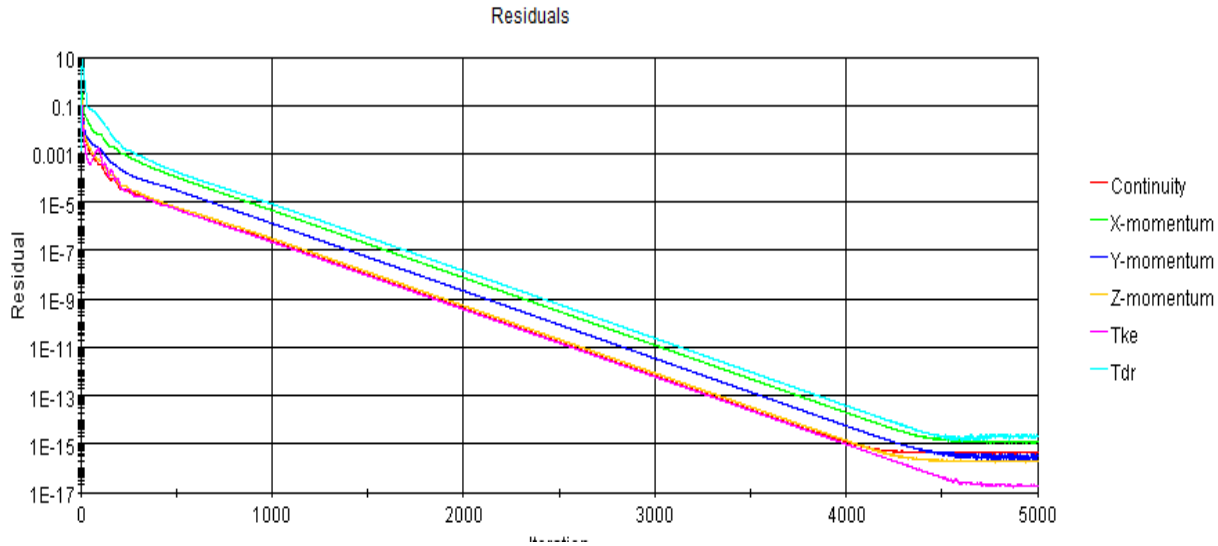

Figure1.3: Residual Plot for Pipe 2

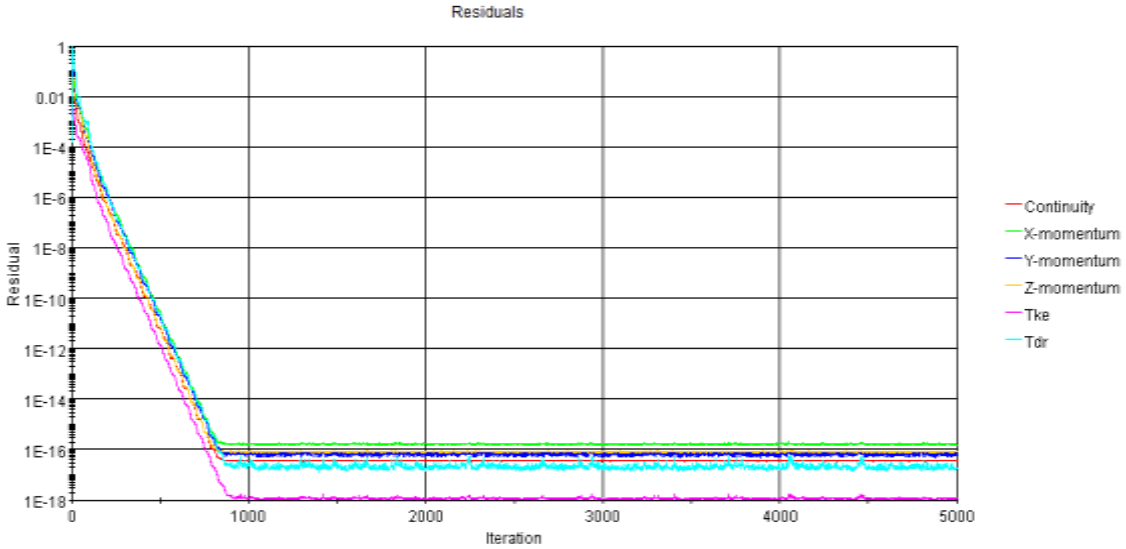

Figure1.3: Residual Plot for Pipe 3

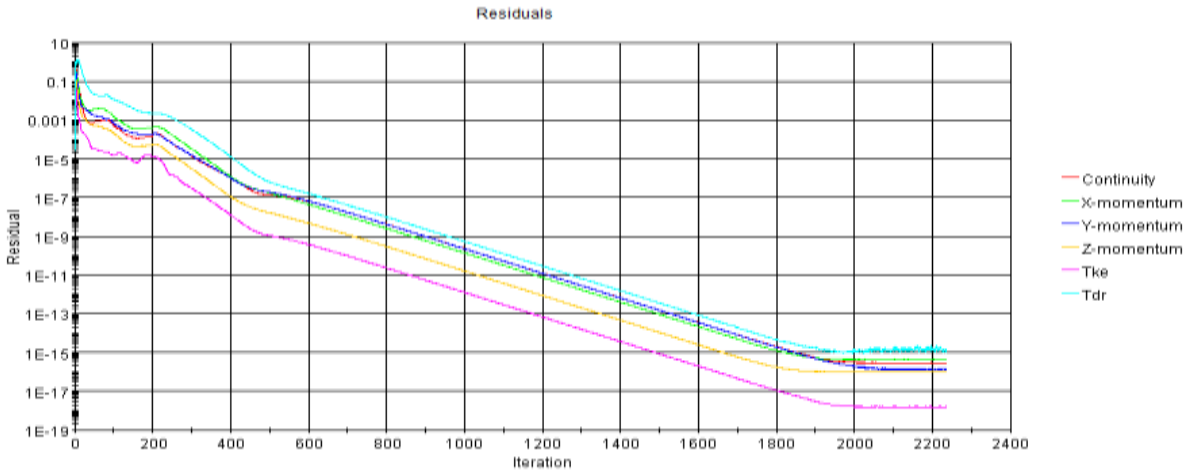

Figure1.5: Residual Plot for Pipe 4

As shown in Figure 1.2, the computation for pipe 1 converges after about 3500 iterations. At this point, the residual values were below 1E-4 as required. In Figure 1.2, the computation for pipe 2 converges after about 4500 iterations. At this point also, the residual values were below 1E-4 as required. For pipe 3, the residual plot shows a convergence after 900 iterations. This is as

DOI: 10.31695/IJASRE.2018.32765

presented in Fig. 3. The residual plot for pipe 4 shown in Fig. 4 converges after 2000 iterations. The convergence point is summarised in Table 1.2.

Table1.2. Convergence Points for the Simulation of different Exit Configurations

Pipe Geometry	Convergence (Iterations)
Pipe 1	3500+
Pipe 2	4500+
Pipe 3	900+
Pipe 4	2000+

As soon as the computations converged, the run were terminated and the values of the different parameters of the flow were observe and recorded from the model. From Table 1.2, it can be deduced that the flow in the exit configuration 3 converges faster. Total pressure is measured at a stagnation point where the fluid velocity is zero and all kinetic energy has been converted into pressure energy (isentropically). For an ideal gas with constant specific heat, it is the addition of static and dynamic pressure. A plot of the total pressure showing the pressure gradient across the pipe of the various pipes is shown in Figure 1.6 to Figure 1.9. From Figure 1.6, the maximum total pressure within the system is 12104Pa. Also, from the pressure plot it is discovered that the pressure remained steady until it reaches the junction where a division of the flow occurs. Since there is no outlet at one pipe end, a back flow occurs that increases the pressure at the junction and forces the flow in the other direction. There is a considerable pressure loss in the system that can be explained by the total work done within the system. It is observable that the exit pressure is stratified with three distinct layers. However, the layer with the highest or maximum pressure has a total pressure relatively lower than the inlet pressure as seen in Figure 1.6.

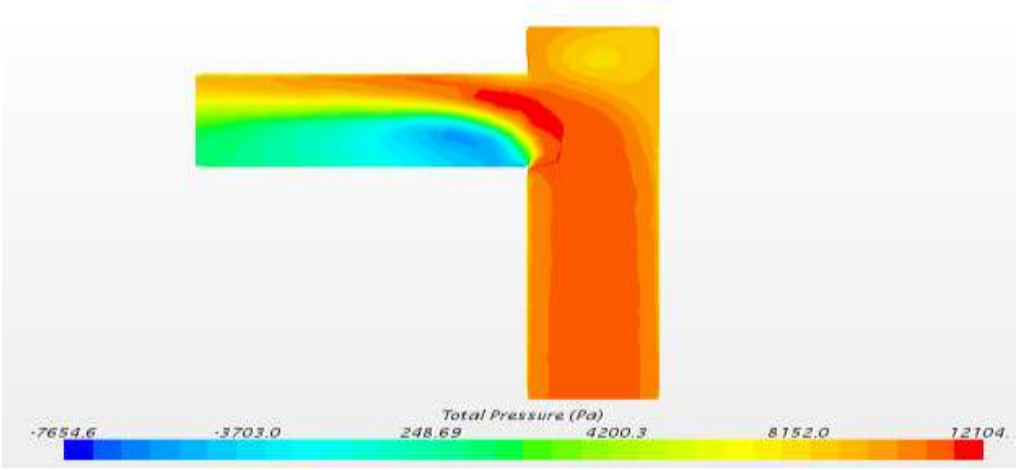

Figure1.6: Plot of Total Pressure for Pipe 1

As shown in Figure 1.7, the maximum total pressure within the system of pipe 2 is 10704Pa. The pressure plot shows a steady pressure from the inlet till it reaches the bend. At the bend, a region of low pressure is created which forces the flow to follow a path closer to the larger side of the bend. A pressure gradient is created and as such the inlet pressure is greater than the outlet pressure.

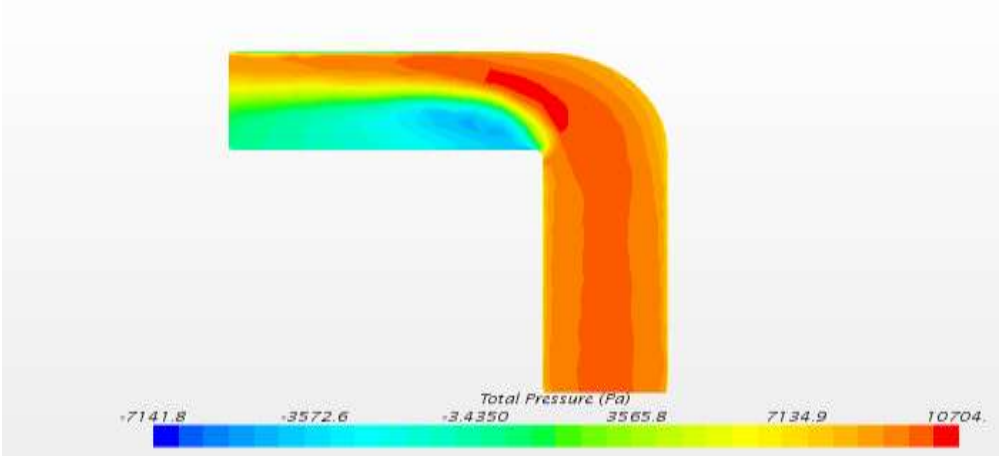

Figure1.7: Plot of Total Pressure for Pipe 2

The total pressure plot for pipe 3 is presented in Figure 1.8 while that of pipe 4 is shown in Figure 1.9.

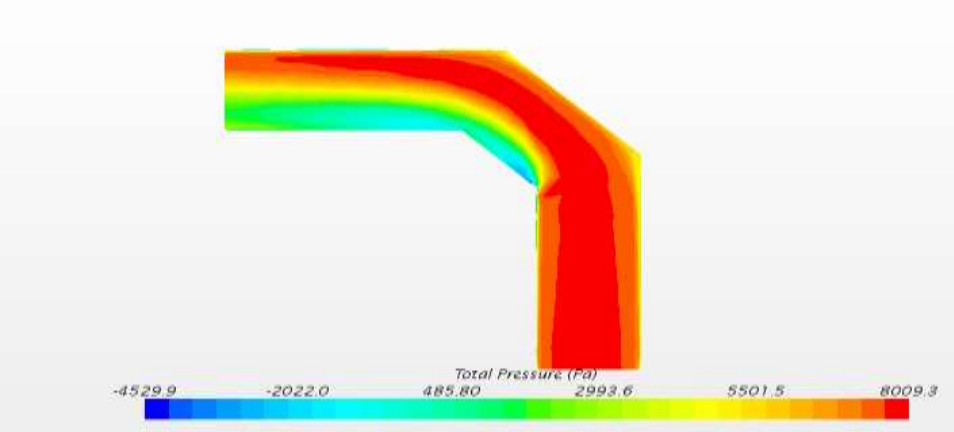

Figure1.8: Plot of Total Pressure for Pipe 3

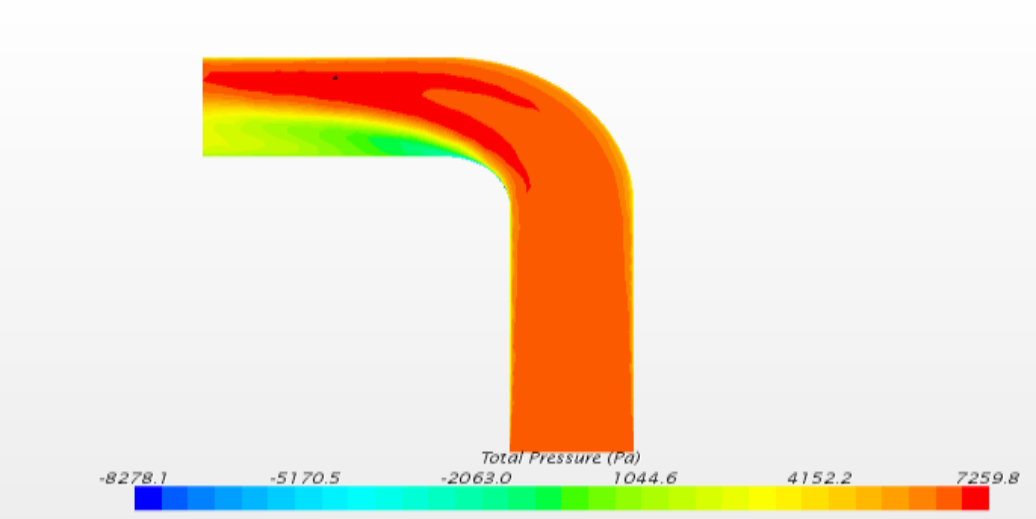

Figure1.9: Plot of Total Pressure for Pipe 4

The values for maximum total pressures in pipe 1-4 show that the pipe exit configuration 4 has the lowest total pressure while the exit configuration 1 has the highest. A common situation in all the exit configuration models is that the total pressure at the inlet is higher than that of the outlet. The flow is therefore made possible by means of difference in pressures. It is worthy of note that for all the exit configurations the boundary layer is not conspicuous. The reaction between the fluid and the wall of the riser are very negligible. To find the inlet static pressure by hand calculation, the equation below is used:

$$\mathbf{P_o = P_{(inlet\ static)} + 0.5(\rho V^2)} \qquad \text{----------(1.1)}$$

Where,
$\mathbf{P_o}$ = Total Inlet Pressure (Pa),
$\mathbf{P}_{(\text{inlet static})}$ = Inlet Static Pressure (Pa).
$\boldsymbol{\rho}$ = Density of the fluid (kg/m^3), **V**: Inlet velocity (m/s).

If the velocity increases, the total pressure at the inlet and the outlet would increase since static pressure is dependent on the velocity of the flow. The static pressure at the inlet and the outlet vary because of the velocity profile in both locations. The static pressure plots in Figure 1.10 to Figure 1.13 show that depending on the exit configurations, regions with high static pressure vary drastically. The difference between the static pressure and the absolute pressure is given as $0.5(\rho V^2)$. The static pressure was maximum at the inlet and least in the outlet. This is evidenced in the static pressure plots for each exit configurations shown in Figure 1.10 to Figure 1.13. For the pipe 1, the static pressure plot showed a pressurised region near the junction on the side of the branch without opening. The pressurised regions show that in cases where this exit configuration is used, the system may experience unnecessary pressure configuration near the close branch. Before the junction however, the pressure distribution in the pipe is relatively even and steady. The pipe may experience some level of vibration because of the large region of negative static pressure which would correlate to very low total pressure at such regions. The static pressure plot for pipe 1 is presented below.

DOI: 10.31695/IJASRE.2018.32765

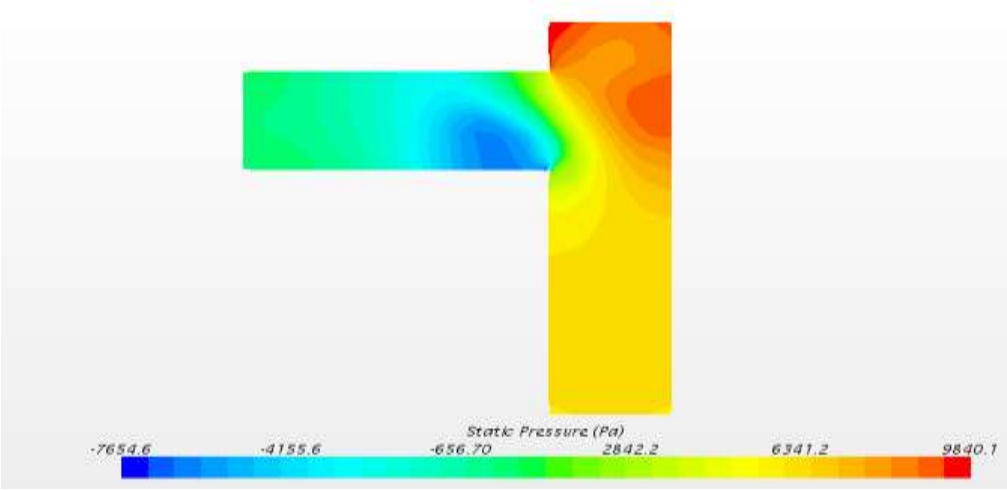

Figure1.10: Static Pressure Plot for pipe 1

As shown in Figure 1.11, the flow in pipe 2 has large regions with negative static pressure and relatively large high pressure region at the bend resulting from fluid particles impacting directly on the corner. The ultimate result of such high pressure gradient is that the flow is forced rather than free at the exit. Another noticeable effect is that the elbow fitting used in real life fails faster that every other part of the pipe. Figure 1.12 representing the flow through pipe 3 is relatively less stressed when compared to other types of flow in the different exit configurations. The sloppy nature of elbow ensures that very minute regions of high and negative static pressures are generated within the flow. This means that the larger portion of the flow moves freely without excessive force which in turn reduces the exposure of the pipe to wear.

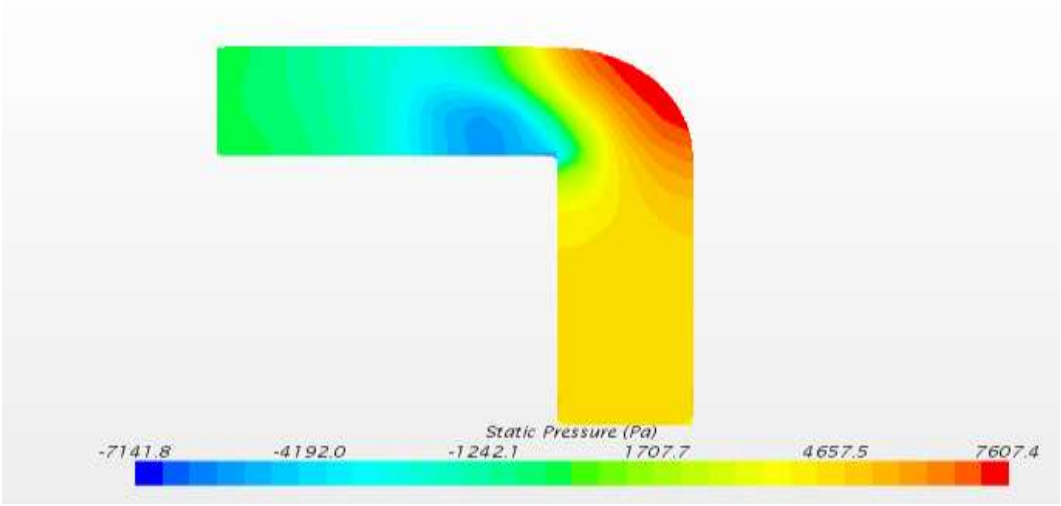

Figure1.11: Static Pressure Plot for pipe 2

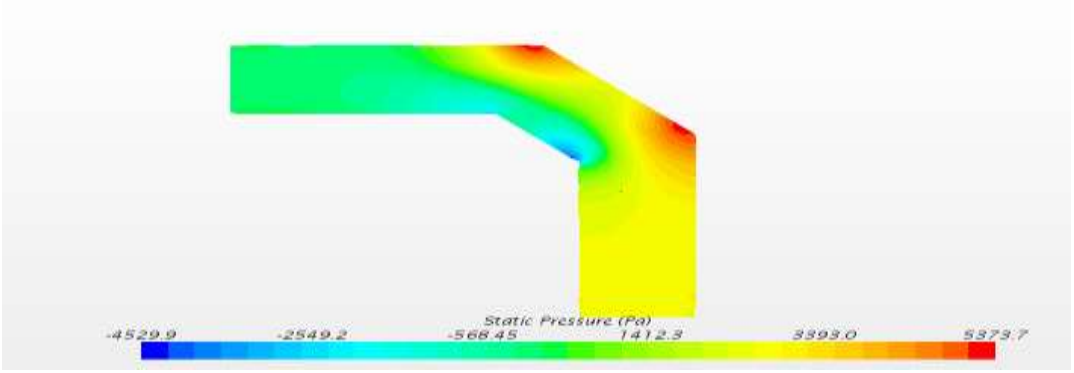

Figure1.12: Static Pressure Plot for pipe 3

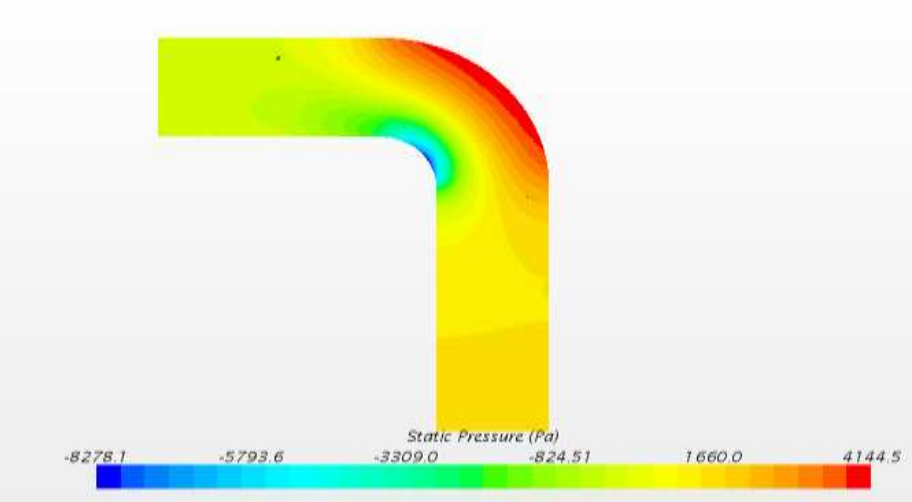

Figure1.13: Static Pressure Plot for pipe 4

In Figure 1.13, the flow is divided into three distinct layers at the elbow. However the region with high static pressure is larger than other layers at the elbow. The values for static pressure in Table 1.3 show that the exit configuration 4 has the lowest static pressure while the exit configuration 1 has the highest. A common situation in all the exit configuration models is that the static pressure at the inlet is higher than that of the outlet. A summary of all the results obtained from the Single phase flow simulation is given in Table 1.3.

Table1.3. Results obtained from the Single Phase Flow Simulation

Pipe	Convergence (Iterations)	Total Pressure (Pa)	Static Pressure (Pa)
1	3500+	12104	9840.1
2	4500+	10704	7607.5
3	900+	8009.3	5373.7
4	2000+	7259.8	4144.5

By considering the number of iterations before the model converges, it is relatively easy to conclude that the model for the exit configuration 3 is the easiest. Companies where the computational cost is of paramount importance would consider the choice of exit 4 if oil-field problems and monitoring are done via CFD tools. The total pressure and the static pressure are low for exit 3 and lowest for exit 4. The differences in the pressure are minimal and can be considered to be insignificant. However, the plots for both static and total pressure must be considered for individuals who regard the pressure within the system as the most important parameter for selection. From all the factors available from the simulation, it is necessary to choose between the third exit configuration and the fourth exit configuration which one is judged to be the best. The concept/criteria matrices method of selection will be used to ease the selection process.

4. CONCLUSION

This research work studied the properties of flow in selected riser exit configurations. The analysis of the flow was carried out as a single phase flow and tried out as a two phase flow gas and crude oil. The various parameters required for detailed study of the flow were computed. The maximum velocity within the pipe in a single phase flow were determined to 3.42 metres per second for an 8 (eight) inch riser pipe. The single phase flow analysis showed that:

i. There is pressure difference between the exit and the inlet of the riser pipe and the pressure difference determines the ease with which the fluid flows in the pipe.
ii. The build-up of pressure within the riser is dependent on the exit configuration.

It is important to note that STAR-CCM+ and CFD codes in general are not capable of predicting the minimum fluidization velocity, as well as the minimum bubbling velocity. The codes are unable to make such predictions because the parameters depend on shape of the particles, surface roughness of the particles, the cohesive nature of the particles and the six distributions.

DOI: 10.31695/IJASRE.2018.32765

REFERENCES

[1] A.E. Ikpe, I. Owunna, P.O. Ebunilo and E. Ikpe, "Feasibility Studies on Offshore Triceratops as Future Offshore Structure Using FMEA Approach." *International Journal of Innovative Research and Development*, vol. 5, no. 6, 2016, pp.104-113

[2] H. Alia, U. Mukhtarb, B. Tijanib, and M. Auwal, "Dynamic relationship of exchange rates and crude oil prices in South Africa: Are there asymmetries." *Research Journal of Finance and Accounting*, vol. 6, no.6, 2015, pp. 195 – 200

[3] V. Batac and M. Tatlonghari, "The Behavior of Exchange Rates, Crude Oil Prices, and Money Supply and their Effects on Philippine Stock Market Performance: A Cointegration Analysis." *Rev. Integr. Bus. Econ. Res.*, vol. 2, no.2, 2013, pp. 60 - 227

[4] N.S. Woo, S.M. Han and Y.J. Kim, "Design of a Marine Drilling Riser for the Deepwater Environment. 11th International Conference on Advances in Fluid Mechanics, 5-7 September, 2016, Ancona, Italy." *WIT Transactions on Engineering Sciences*, vol. 105, 2016

[5] D. Zhang, Y. Chen and T. Zhang, "Floating Production Platforms and their Applications in the Development of Oil and Gas Fields in the South China Sea." *Journal of Marine Science and Application*, vol. 13, no. 1, 2014, pp. 67-75

[6] S. Kyriakides and E. Corona, Mechanics of Offshore Pipelines, Volume 1: Buckling and Collapse, Elsevier Science, Oxford, UK and Burlington, Massachusetts, 2007.

[7] B.Yong, and B. Qiang, Subsea Pipelines and Risers 1st Edition. Elsevier Science, ISBN: 9780080445663, 2005

[8] D. Walter, D. Thomas and S. Hatton, Design and Optimization of Top Tension Risers for Ultra Deep Water. Floating Production System, Conference, 2004

[9] J. Guesnon, C. Gaillard and F. Richard, "Ultra Deep Water Drilling Riser Design and Relative Technology." *Oil and Gas Science and Technology*, vol. 57, no.1, 2002, pp. 39-57

[10] H. Devold, Oil and Gas Production Handbook: An Introduction to Oil and Gas Production, Transport, Refining and Petrochemical Industry. ABB Oil and Gas, Edition 3.0, ISBN: 9788299788632, 2013

[11] A.E. Ikpe and E.K. Orhorhoro, "Pressure Losses Analysis in Air Duct Flow Using Computational Fluid Dynamics (CFD)." *International Academic Journal of Science and Engineering*, vol. 3, no.9, 2016, pp. 55-70

[12] E.K. Orhorhoro, A.E. Ikpe and Y. Oloke-Ehisuan, "Flow Computation of Total Head Losses and Total Pressure Losses in a Typical Gasoline Fuel Injector System." *International Academic Journal of Science and Engineering*, vol. 3, no. 10, 2016, pp.30-47

[13] A.E. Ikpe, E.K. Orhorhoro and O.G. Ogiemudia, "Computational Fluid Dynamics (CFD) Simulation in Air Duct Channels Using STAR CCM+. *European Journal of Advances in Engineering and Technology.*" vol. 4, no.3, 2017, pp.216-220